Annals of Biomedical Engineering (© 2013)
DOI: 10.1007/s10439-013-0752-3

BMES BIOMEDICAL ENGINEERING SOCIETY™ www.bmes.org

Methods for Measuring Right Ventricular Function and Hemodynamic Coupling with the Pulmonary Vasculature

ALESSANDRO BELLOFIORE and NAOMI C. CHESLER

Department of Biomedical Engineering, University of Wisconsin-Madison, 2146 Engineering Centers Building, 1550 Engineering Drive, Madison, WI 53706, USA

(*Received 31 August 2012; accepted 21 January 2013*)

Associate Editor Ender A Finol oversaw the review of this article.

Abstract—The right ventricle (RV) is a pulsatile pump, the efficiency of which depends on proper hemodynamic coupling with the compliant pulmonary circulation. The RV and pulmonary circulation exhibit structural and functional differences with the more extensively investigated left ventricle (LV) and systemic circulation. In light of these differences, metrics of LV function and efficiency of coupling to the systemic circulation cannot be used without modification to characterize RV function and efficiency of coupling to the pulmonary circulation. In this article, we review RV physiology and mechanics, established and novel methods for measuring RV function and hemodynamic coupling, and findings from application of these methods to RV function and coupling changes with pulmonary hypertension. We especially focus on non-invasive measurements, as these may represent the future for clinical monitoring of disease progression and the effect of drug therapies.

Keywords—Ventricular–vascular coupling, Right ventricular dysfunction, Mechanical efficiency, Metabolic efficiency, Pulmonary circulation, Pulmonary hypertension.

INTRODUCTION

The structure and physiology of the right ventricle (RV) are well-matched to the distinctive features of the pulmonary circulation. While the left ventricle (LV) and the systemic circulation serve the entire body, the RV and pulmonary circulation serve only the lung. The pulmonary circulation has shorter arteries and veins, more distensible large arteries and a larger number of peripheral arteries than the systemic circulation.[79] As a result, the pulmonary circulation exhibits low resistance and high compliance, which respectively maintain mean and pulse pressure lower than in the systemic circulation. The resistance and compliance of the pulmonary vasculature contribute to the right ventricular afterload, which comprises the steady and unsteady loads that oppose the ejection of blood during ventricular systole. The RV afterload is lower than the LV afterload, both in terms of mean and pulsatile loads.[98] Ideally, the systolic function of each ventricle dynamically adapts to the afterload, a concept called "ventricular–vascular coupling".[89]

Efficient right ventricular–pulmonary vascular coupling is thought to maintain cardiac output (CO) while maximizing the mechanical efficiency of the RV. Many cardiopulmonary diseases, such as pulmonary arterial hypertension (PAH) compromise RV function, in particular its ability to increase contractility sufficiently to preserve efficient coupling with the diseased pulmonary vasculature. In patients with chronic cardiopulmonary disease, life expectancy and quality of life could be dramatically improved by therapeutic approaches aimed at preserving or restoring RV function and efficiency of coupling with the pulmonary vasculature. On the one hand, development of effective treatment strategies relies on a better understanding of the mechanisms of RV dysfunction. On the other hand, selection of the best therapy for each patient may require frequent monitoring of RV function, ideally in a non-invasive fashion.

One challenge for biomedical engineers is to develop better, non-invasive methods for measuring RV function and efficiency of hemodynamic coupling, which is the subject of this review. In the first part ("Physiology and Mechanics of the RV" section), we examine how the RV works, the emphasis being on the key differences between the left and RVs. In the second part

Address correspondence to Naomi C. Chesler, Department of Biomedical Engineering, University of Wisconsin-Madison, 2146 Engineering Centers Building, 1550 Engineering Drive, Madison, WI 53706, USA. Electronic mail: chesler@engr.wisc.edu

Published online: 20 February 2013

("Methods for Measuring RV Function" section), we review established and novel methods for measuring RV function and right ventricular–pulmonary vascular coupling efficiency. In the third part ("RV Dysfunction in Pulmonary Hypertension" section), we provide examples of how these methods can be used to investigate RV dysfunction and failure in particular due to pulmonary vascular disease.

PHYSIOLOGY AND MECHANICS OF THE RV

The RV is not the LV

Historically, the RV has been paid less attention than the LV. The lower pressures it must generate make it less prone to dysfunction and valvular diseases. However, progression of RV dysfunction to failure occurs in a number of diseases, including pulmonary hypertension, and is frequently fatal. When in the last decades awareness increased about the importance of the pathophysiology of the RV and the pulmonary circulation, it appeared convenient to adopt methods and metrics already established for the LV and systemic hypertension. However, despite the obvious similarities between the left and the right sides of the heart, some remarkable differences exist, and these differences can make the use of LV-based metrics impractical in the RV or the results questionable.

The RV is a crescent-shaped chamber that wraps around the LV. The complex shape makes estimation of volumes and surface areas challenging. The RV free wall is thinner than the LV free wall as a consequence of the lower ventricular pressures (Laplace's law). The crescent shape and the thin wall make the RV ventricle more compliant than the LV.[54] Additional differences in physiological and pathological ventricular response to afterload may derive from the coarser pattern of apical trabeculation in the RV[4] (Fig. 1).

Furthermore, RV pressure changes correlate with RV volume changes over the cardiac cycle differently than LV pressure changes correlate with LV volume changes. Pressure–volume (PV) loops are convenient representations of these correlations and have been used extensively to evaluate ventricular contractility, arterial afterload and ventricular–vascular coupling in the RV.[14,30,46,48,92,99] The term contractility (or, equivalently, inotropy) has been used in the literature to loosely indicate either a property of isolated muscle cells (myocardial contractility) or a state of the whole organ (ventricular contractility).[6] Since ventricular contractility can be measured *in vivo*, in this review we will refer to ventricular contractility, unless otherwise specified. In the PV plane, the PV loop is confined between two curves: the end-systolic pressure–volume relationship (ESPVR) and end-diastolic pressure–volume relationship (EDPVR). The ESPVR is approximately a straight line in a range of physiological conditions. The slope of the ESPVR is the end-systolic elastance, a measure of RV contractility. The EDPVR is tangent to the PV loop at its end-diastolic point and is a measure of

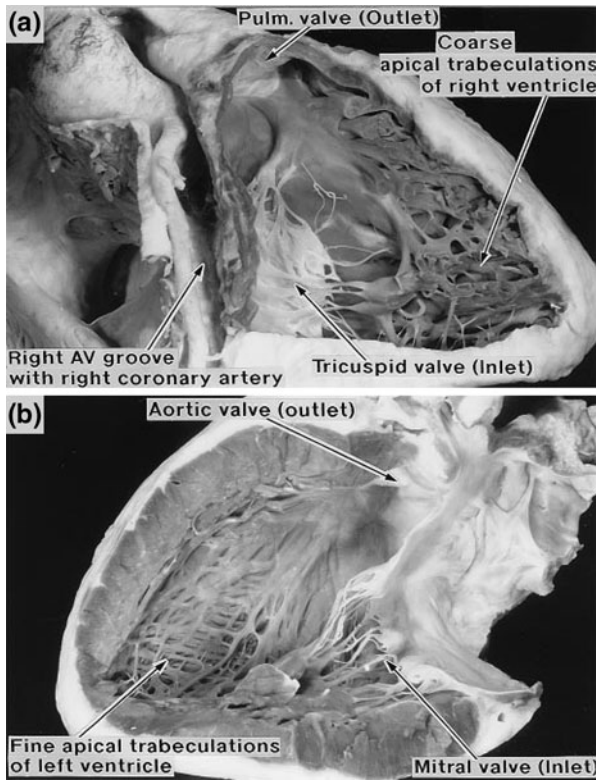

FIGURE 1. Comparison of the apical trabeculation patterns in the RV (top) and the LV (bottom). Reprinted from Anderson and Ho[4] with permission from Elsevier.

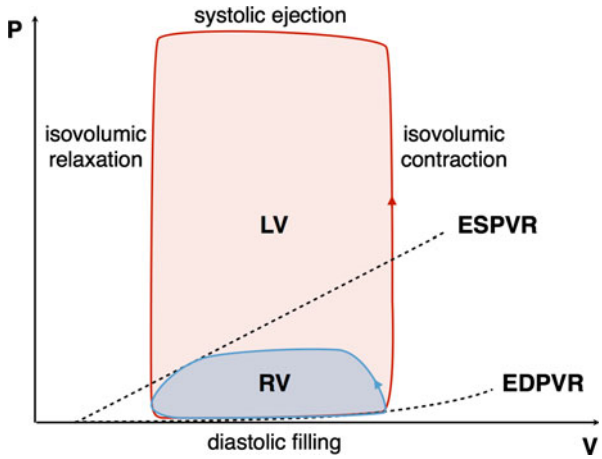

FIGURE 2. Sketch of the PV loop in the RV (blue) and LV (red). The pressure variation in the RV is much lower, whereas the two ventricles pump the same SV. The dashed lines are the ESPVR and EDPVR for the RV PV loop.

ventricular compliance at maximum filling. Example PV loops are sketched in Fig. 2.

The end-systolic pressure (ESP) in the LV is approximately six times higher than in the RV. Nevertheless, the two ventricles pump the same stroke volume (SV). In the following, acronyms of ventricular volumes and pressures will refer to the RV, unless otherwise specified. In the LV, the four stages of the heart cycle (systolic ejection, isovolumic relaxation, diastolic filling, isovolumic contraction) are easily discernible, because the shape of the PV loop is approximately rectangular. In contrast, in the RV the isovolumic stages, and in particular the isovolumic relaxation, are not well-defined and the RV PV loops are trapezoidal or triangular in shape.[10,82] The non-rectangular shape makes it more difficult to identify the end-systolic point, which results in a higher degree of uncertainty in the estimation of the slope of the PV relationship at end systole, as compared to the LV.

As a consequence of these structural and functional differences between the RV and the LV, established knowledge on the LV response to pathological increases in pressure or volume cannot be directly translated to the RV. In addition, these differences warrant caution in applying results from the LV to the study of the RV.

Mechanisms of RV Function Autoregulation

An important similarity between the ventricles is that each can regulate its contraction in response to variations in afterload and preload, although not entirely independently. In the myocardium, muscle fibers are stretched during diastole. The term preload indicates the load imposed on the fiber by the end of diastole and is proportional to the maximum elongation of myocardial fibers. During systole, myocardial fibers contract against an increasing load, due to the rise in ventricular pressure. The additional load imposed on myocardial fibers by the pressure increase during contraction is called afterload. The contracting fibers develop a tension that depends on the initial length of the fibers and on the inotropic state of the myocardium. Figure 3 illustrates the length–tension diagram for myocardial fibers. Each curve represents the length–tension dependence for a given inotropic state. If the initial length of the fibers is increased (moving from point A to B), a greater tension is generated and the fibers contract at a faster rate. Therefore, as a result of an increase in preload at constant heart rate, myocardial fibers shorten to a greater extent. The diagram in Fig. 3 shows that the tension of the myocardial fibers can also change independently of fiber initial length. Length-independent changes in fiber tension represent changes in the inotropic state of the myocardium. If myocardial inotropy is increased (from point B to C in Fig. 3), the length–tension curve shifts so that a larger tension is developed for a given preload.

In the RV, two autoregulation mechanisms act to preserve cardiac function when afterload or preload are altered. Here "autoregulation" means that the mechanisms are intrinsic to the cardiac muscle cells, independent of external (hormonal or nervous) input. Heterometric autoregulation is based on the Frank-Starling mechanism and is an immediate response to a change in preload. According to this mechanism, an increase in end-systolic volume (EDV) produces an equal increase in SV that restores normal end-systolic volume (ESV). Heterometric autoregulation reflects, at organ level, length-dependent changes in myocardial contraction.

Homeometric autoregulation, based on the Anrep effect,[56] is an inotropic mechanism of response to increased afterload. According to this mechanism, the ventricle responds to an increase in afterload with an increase in myocardial inotropy. An increase in afterload impairs the ability of the ventricle to eject blood, so the SV decreases. In homeometric autoregulation, the increase in inotropy produces a compensatory increase in SV. Homeometric autoregulation reflects, at organ level, length-independent changes in myocar-

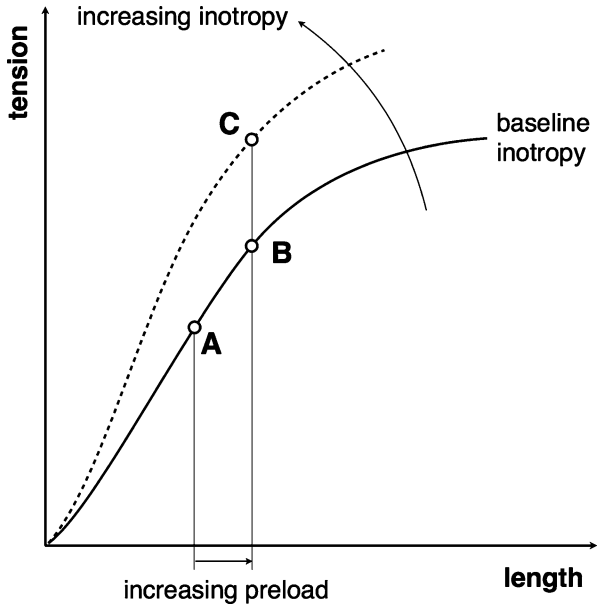

FIGURE 3. Length–tension diagram for myocardial fibers. The solid line represents the length–tension relationship at baseline inotropy. An increase in maximum fiber elongation at end diastole (preload) produces an increase in fiber tension (from point A to B), resulting in a stronger contraction. If inotropy is increased, the length–tension curve is shifted upward and to the left (dashed line). An increase in inotropy (from point B to C), produces in an increase in fiber tension independent of fiber length.

dial contraction. It is important to note that homeometric autoregulation is a slower mechanism than heterometric regulation, with a response time on the order of minutes.

A visual representation of these two mechanisms in the PV plane is illustrated in Fig. 4. In the heterometric response to increased preload (Fig. 4, left plot), an increase in EDV is compensated for by an increase in SV, so that normal ESV is restored without changes in ventricular inotropy or ESP. Heterometric autoregulation can also be triggered by an increase in afterload. As illustrated in Fig. 4 (center plot), an increase in ESP (afterload) would increase ESV, thus reducing SV. Normal SV is restored by an increase in EDV, consistent with the Frank-Starling mechanism. In homeometric autoregulation (Fig. 4, right plot), the RV compensates for an increase in ESP by increasing ventricular inotropy, so that normal SV is restored without altering the preload. In actuality, an increase in afterload induces an immediate heterometric response, which enables accommodation of the pressure increase by shifting the RV working condition towards larger volumes. As soon as the homeometric autoregulation becomes effective, the increase in contractility allows for the normalization of EDV. If systolic function cannot be enhanced any further, RV dilatation remains the only effective response to increased afterload.

Measures of ventricular contractility and volume changes in response to afterload and preload changes can help evaluate RV autoregulation activity and, as such, represent important end-points in the clinical monitoring of RV function.

Hemodynamic Coupling, Mechanical and Metabolic Efficiency of the RV

RV function relies on hemodynamically efficient interactions with the pulmonary circulation, proper functioning of myocardial cells and tissues and LV function as well. With regard to the latter, in the healthy heart, the RV and LV contract and relax synchronously. Since the workload of the RV is significantly lower than the LV, the RV can benefit from the LV systolic contractions. It is estimated that in normal conditions LV contractions contribute to 20–40% of the RV pressure increase.[75]

When considering how the function of the ventricle is paired to its circulation, the concept of ventricular–vascular coupling (or hemodynamic coupling) is typically evoked. This concept was originally postulated in the context of a mechanical characterization of the LV.[89] The ventricle and the arterial system are treated as elastic chambers, and the properties of each are described in similar dimensions ($ML^{-4}\,T^{-2}$) or units (mmHg/mL or N/m^5). Sunagawa *et al.*[89] chose to define each in terms of an elastance, or a change in pressure per unit change in volume. Thus, the ventricular elastance when measured at the end of the ejection phase is the end-systolic elastance (E_{es}) and is equal to the slope of the ESPVR. The vascular elastance, typically called the effective arterial elastance

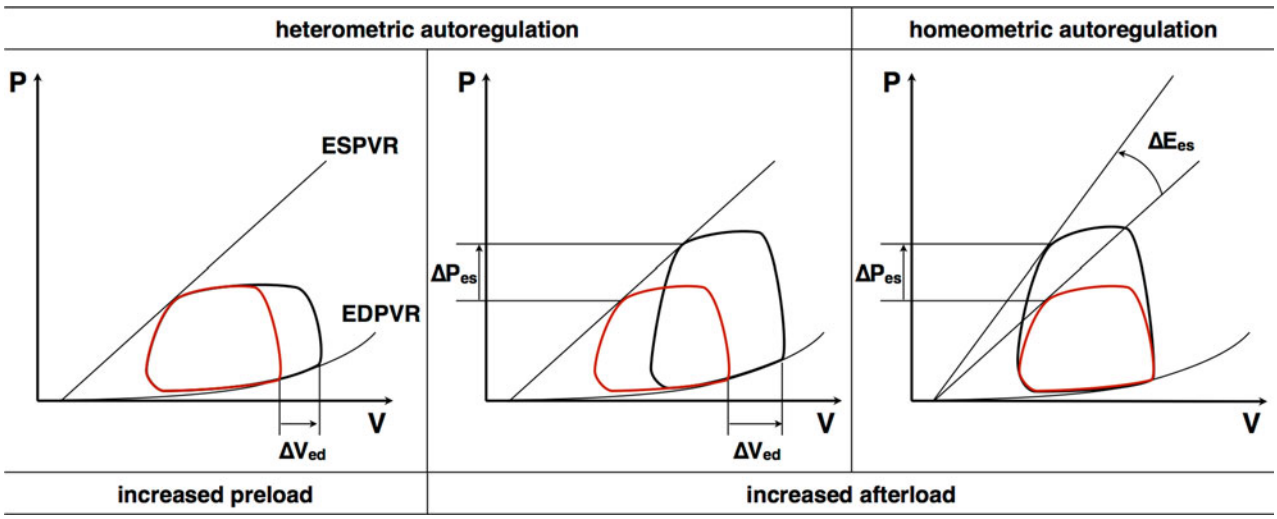

FIGURE 4. Representation of heterometric (left and center plot) and homeometric autoregulation (right plot). If preload is increased (left plot) heterometric autoregulation increases SV by the same ΔV_{ed}. If afterload is increased, both heterometric and homeometric responses are activated. In heterometric autoregulation (center plot), an increase in EDV (ΔV_{ed}) leads to an increase in pressure (ΔP_{es}) with no change in SV and inotropy. In homeometric autoregulation (right plot), a pressure increase (ΔP_{es}) to match increased afterload is achieved by increasing RV contractility (ΔE_{es}) with no change in SV and preload. The baseline loop is sketched in red. The ESPVR line and the EDPVR line define the limits of RV working conditions.

E_a, is derived from a three-element Windkessel model of the arterial system and has same units as E_{es}. It is postulated that end-systolic ventricular elastance and vascular elastance are dynamically adjusted in order to maintain optimal coupling. Experimental evidence and theoretical considerations have suggested that optimal coupling guarantees that most RV pump energy is transferred to the blood flow.[16] Ventricular and vascular elastances can be altered by certain pathologies, in which case the hemodynamic coupling can be less than optimal. In order to quantify how far the ventricular–vascular interactions are from ideal coupling, the hemodynamic coupling efficiency η_{vv} is defined as

$$\eta_{vv} = \frac{E_{es}}{E_a} \quad (1)$$

Assessment of ventricular and arterial elastances in animal and clinical research studies has demonstrated that coupling efficiency is significantly different in the healthy and diseased states. It is generally accepted that η_{vv} is larger than unity in healthy subjects,[26,46,78] whereas values of η_{vv} close to or lower than unity occur with disease.[26,47,78] However, reference ranges for η_{vv} may depend on the formulations used to calculate E_{es} and E_a.

The mechanical efficiency of the RV itself can be defined in several ways. If 100% efficiency were possible, all energy input into the ventricle would be transformed into useful mechanical work. In fact, the contractile power generated by the myocardium is in part turned into hydraulic power (actually transferred to the blood flow) and in part spent to store energy in the elastic ventricular tissues during diastole and overcome friction between blood and tissues.[1,21] Of the hydraulic power, only a fraction contributes to the net forward blood flow (steady power) with the rest spent on oscillations in blood flow (oscillatory power). Myocardial activity generates the total power, which itself is fueled by O_2 consumption. Therefore, if we define the steady hydraulic work done as the useful mechanical work for the circulation, cardiac mechanical efficiency can be defined as the ratio of the steady hydraulic power to the total power generated by myocardial O_2 consumption.[94,100] For the LV it has been hypothesized that physiological working conditions achieve maximal cardiac efficiency rather than maximal output power.[16] That would ensure the ventricle has a reserve stroke work that can be recruited, for instance, during physical exercise. A similar capability to use a contractile reserve to increase stroke work has been observed in the RV.[34]

Another measure of the efficiency of the RV can be defined as the ratio of steady hydraulic power to oscillatory plus steady power, although this is really the efficiency of hydraulic power generation for the RV. Steady hydraulic power, typically calculated as the product of the mean pulmonary artery pressure (mPAP) and CO, must overcome pulmonary vascular resistance (PVR) to move blood through the lungs. The oscillatory power produces zero-mean oscillations in the flow, the amplitude of which depend on arterial compliance. Compliance determines the way in which pressure and flow waves propagate in the pulmonary vasculature, with stiffer arteries enhancing wave reflections and increasing the pulsatile load on the ventricle.

Since the ratio of steady to steady-plus-oscillatory power depends on pulmonary vascular resistance and compliance, both measures of RV efficiency defined here depend on pulmonary vascular resistance and compliance. Also, both measures of RV efficiency provide useful information on how altered preload and afterload affect the energetic response of the RV where increasing inefficiency may be a sign of progressive RV dysfunction.

Metabolic efficiency refers to the ability to generate power with a minimum consumption of energy substrate (mostly glucose and fatty acids) in the cells and tissues. In this sense, power can be generated by either glucose and fatty acid oxidation or glycolysis. Glucose oxidation yields more ATP than glycolysis, and so it has a higher metabolic efficiency,[95] whereas glycolysis consumes no O_2. In the RV energy balance, the power required to contract the ventricle and pump blood into the pulmonary circulation must be matched by the power generated in the myocardium. Crucial for RV performance is the balance between O_2 demand and supply. O_2 demand can increase physiologically if a higher CO is required (such as during physical exercise) or in the presence of a pathological increase in pressure. In general an increased O_2 demand can be accommodated by increasing either the fraction of O_2 extracted from blood or myocardial perfusion. If the energy demand exceeds O_2 and myocardial blood flow reserve, the RV becomes ischemic. Faced with a lack of oxygen, the RV is forced to switch its mitochondrial metabolism from glucose and fatty acid oxidation to glycolysis,[49] with a subsequent decrease in RV metabolic efficiency. This metabolic switch is often reversible, however. Optimal metabolic efficiency is restored when, for example after physical exercise, the O_2 demand returns to normal levels. Chronic reduction of metabolic efficiency may impair the ability of the RV to accommodate increases in afterload.[19,67] Therefore, measurements of RV metabolic efficiency *via* assessment of glucose and O_2 consumption in the RV myocardium may help clarify mechanisms of RV dysfunction and failure.

Methods for measuring hemodynamic coupling and mechanical efficiency of the RV are based on

either PV analysis ("Pressure–Volume Loop Analysis" section) or pressure-flow analysis ("Pressure-Flow Analysis" section). Metabolic efficiency can be assessed non-invasively with positron emission tomography ("Measurements of Metabolic Efficiency" section). Further methods for monitoring RV function non-invasively are based on measures of RV volumes ("RV Volumes" section), RV fibrosis ("RV Wall Stress and Myocardial Fibrosis" section) and RV deformation ("RV Deformation" section). Finally, non-invasive measurements of pulmonary artery compliance ("Relative Area Change of the Proximal Pulmonary Arteries" section) can be used to indirectly monitor RV function.

METHODS FOR MEASURING RV FUNCTION

Invasive Measurements of RV Function and Efficiency

Invasive right heart catheterization (RHC) is typically required to measure pressure in the RV and pulmonary vasculature; it can also be used to measure CO. From measurements of mPAP, pulmonary capillary wedge pressure (PCWP) and CO, PVR can be calculated as

$$\mathrm{PVR} = \frac{\mathrm{mPAP} - \mathrm{PCWP}}{\mathrm{CO}} \tag{2}$$

where PCWP is used to approximate left atrial pressure (LAP). PVR has units of Pa s m^{-5} (or dyn s cm^{-5}). Since pressures are measured in mmHg and CO has units of L/min, in the clinical practice PVR is usually expressed in Woods units (mmHg min/L). Pulmonary artery pressures can also be estimated non-invasively from the tricuspid valve regurgitation velocity and application of a simplified form of the Bernoulli equation. While this is a widely used technique, significant discrepancies have been found between invasive measurements and non-invasive estimates of pressure.[23,31,71] Thus, pressures measured from RHC remain the gold standard for measuring RV function and efficiency.

Although measurements of pressure and PVR are an important diagnostic tool for pulmonary vascular disease, these metrics alone do not provide sufficient insight into RV function and have a limited prognostic value.[28,90,97] However, they can be combined with either volume or flow measurements to assess hemodynamic coupling and mechanical efficiency of the RV.

Pressure–Volume Loop Analysis

Analysis of simultaneous RV pressure and volume data can provide a detailed evaluation of RV function. Measurements of hemodynamic coupling and efficiency of the RV, obtained from PV analysis, have been demonstrated to be sensitive to pulmonary vascular disease and its progression.[26]

The main challenge in measuring ventricular–vascular coupling, which is typically done from PV loops, is the assessment of RV contractility from E_{es} (ESPVR). The most accurate method requires generating multiple PV loops while varying RV preload. This is achieved by quick occlusion of the inferior vena cava with an inflated balloon.[37] As ventricular contractility is approximately independent of preload, it can be calculated by fitting a straight line through the end-systolic points (Fig. 5, *left plot*). The straight line represents the ESPVR and the intercept with the horizontal axis represents the theoretical volume V_0 of the unloaded ventricle. The use of a conductance catheter for simultaneous PV measurements and the need for an occlusion maneuver to vary preload have heavily limited this method, de facto restricting its use to animal models.[30,47,59,70] In humans, conductance catheters have been used only in a limited number of research studies, mostly in the LV.[40,93] Instead of using a conductance catheter, volumes can be measured either by magnetic resonance imaging (MRI), ideally performed simultaneously with RHC,[46] or by integration of a flow waveform obtained during RHC.[26,42,99]

Single-beat methods have been proposed to overcome the need for inferior vena cava occlusion and therefore represent an attractive solution for estimating RV contractility.[64] These methods aim to estimate the ESPVR from a single PV loop.[14] The first assumption required to do so is that a ventricular contraction without ejection (isovolumic contraction) would have the same ESPVR as a normal ejecting beat. In an isovolumic beat, the ESP would reach the highest possible value (P_{max}) for a given contractility. Further assumptions of single-beat methods are that the pressure waveform of an isovolumic contraction can be approximated by a sine wave and that the sine wave best fit to the isovolumic contraction can be extrapolated from normal ejecting beats. Several extrapolation algorithms have been proposed. Then, P_{max} is estimated as the peak value of the sine wave. Finally, the ESPVR is calculated as the straight line through the end-systolic point of the normal ejecting beat and the end-systolic point of the isovolumic beat (EDV, P_{max}), as shown in Fig. 5 (center plot). Although single beat methods have been extensively used to evaluate contractility and η_{vv},[42,65,73,99] their accuracy in the RV has been questioned.[13,44,48]

Contractility can be also estimated from a single PV loop by using a simplified approach borrowed from LV analysis.[88] In this approach, the ESPVR is approximated with the straight line connecting the origin of the PV plane and the point of the PV loop

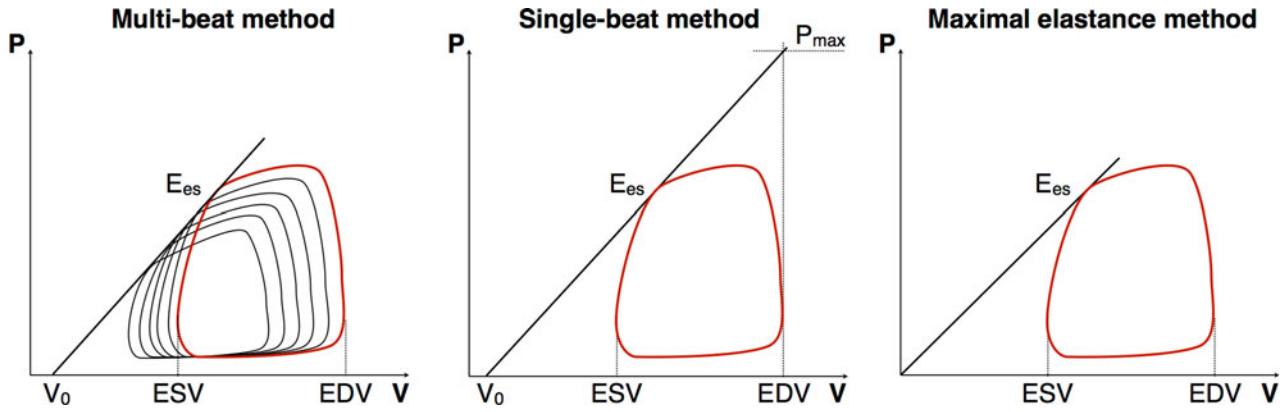

FIGURE 5. Comparison of the methods to evaluate end-systolic elastance from PV loops. Left plot: multi-beat method. Multiple loops are collected while reducing preload and the ESPVR is obtained as the straight line through all the end-systolic points. The loop at baseline preload is sketched in red color. Center plot: single-beat method. The ESPVR is the straight line through the end-systolic point of the single loop collected and the end-systolic point of an isovolumic beat (EDV, P_{max}). Right plot: maximal elastance method. E_{es} is approximated as the maximum pressure-to-volume ratio reached in a single beat. As a result, the ESPVR is the straight line through the origin and the point of the loop where P/V is largest.

with the maximum P/V value. The end-systolic elastance E_{es} is then calculated as the maximal elastance E_{max}:

$$E_{\max} = (P/V)_{\max} \tag{3}$$

The underlying assumption is that the volume V_0 can be neglected[15] (Fig. 5, right plot). This approach has been recently used to propose a noninvasive method to estimate η_{vv} from cardiac MRI.[78]

The effective arterial elastance E_a was originally defined as a steady-state parameter that incorporates the principal elements of the Windkessel model of the vascular bed.[89] By analogy with the formulation used in the systemic circulation, E_a can be estimated as

$$E_a = \frac{\mathrm{mPAP}}{\mathrm{SV}} \tag{4}$$

However, it has been shown that taking into account the LAP provides a better approximation of E_a than the formula in Eq. (4).[59] If the PCWP is taken as an approximation of the LAP as above, the effective arterial elastance can be calculated as:

$$E_a = \frac{\mathrm{mPAP} - \mathrm{PCWP}}{\mathrm{SV}} \tag{5}$$

Accurate measurement of E_{es} and E_a requires complex invasive procedures. In the LV these parameters can be approximated as

$$E_{es,LV} = \frac{\mathrm{ESP_{LV}}}{\mathrm{ESV_{LV}}} \tag{6}$$

and

$$E_{a,LV} = \frac{\mathrm{ESP_{LV}}}{\mathrm{SV_{LV}}} \tag{7}$$

where the subscript "LV" indicates quantities measured in the LV. As a consequence the coupling efficiency in the LV can be estimated non-invasively as

$$\eta_{vv,LV} = \frac{\mathrm{SV_{LV}}}{\mathrm{ESV_{LV}}} \tag{8}$$

This approach has been adapted to the RV,[78] under the further assumption of negligible PCWP. Since this model overestimates E_a, its validity in the RV needs to be further tested.[8]

A measure of ventricular mechanical efficiency ε can be derived from PV loops as

$$\varepsilon = \frac{\mathrm{SW}}{\mathrm{PVA}} \tag{9}$$

where SW is the stroke work (the area of the PV loop) and PVA is the so-called pressure–volume area (PVA). PVA is the area delimited by the ESPVR line, the EDPVR line and the portion of PV loop between end diastole and end systole. In the LV, PVA is linearly correlated with myocardial O_2 consumption,[60] which justifies its use in a measure of mechanical efficiency. Although PVA has been used also in the RV as a measure of O_2 consumption,[70] to the best of our knowledge there is no evidence that the linear relationship found in the LV is valid in the RV.

Pressure-Flow Analysis

Analysis of combined pressure and flow measurements can provide important information about RV hydraulic power and the steady to steady-plus-oscillatory power ratio. Simultaneous pressure and flow data can be acquired placing a fluid-filled catheter in the

main pulmonary artery (MPA) and a non-restricting perivascular flow probe around MPA. This method is used as a research tool for open-chest animal studies.[14,70] In the clinical setting, RHC can be combined with echocardiography to acquire simultaneous MPA pressure and flow waveforms.[39]

Pulmonary vascular impedance (PVZ) defines the relationship between pressure and flow in the MPA. While PVR is responsible for the steady load associated with the net forward blood flow, PVZ includes both the steady and pulsatile components of RV afterload. Fourier analysis of pressure and flow waveforms yields modulus and phase of PVZ, both as functions of frequency f. The value Z_0 of PVZ modulus at $f = 0$ represents a measure of the total PVR, defined as

$$\mathrm{tPVR} = \frac{\mathrm{mPAP}}{\mathrm{CO}} \tag{10}$$

The value Z_c for $f \rightarrow \infty$ (characteristic impedance) is related to proximal arterial stiffness.[61] In the systemic circulation, Z_0 and Z_c reflect the effects of distal arteries and aorta, respectively, on the pressure–flow relationship. Such separation is less clear in the pulmonary circulation, as the distal vasculature contributes significantly to total compliance.[80]

The pressure-flow data can be used to assess the components of the hydraulic power generated by the RV. If MPA pressure and flow waveforms are measured, the total hydraulic power W_{tot} can be calculated combining pressure and kinetic power[24]:

$$W_{\mathrm{tot}} = \frac{1}{T}\int_0^T \left(p(t) + 0.5\rho v^2(t)\right)Q(t)dt \tag{11}$$

where p, v and Q are instantaneous pressure, velocity and flow rate in the MPA, respectively, ρ is blood density and T is the heartbeat duration. In the RV, the kinetic term in Eq. (11) is much smaller than the pressure component and can be neglected.

The mean power output W_{mean} throughout the cycle can be calculated as[35,81]

$$W_{\mathrm{mean}} = \mathrm{mPAP} \times \mathrm{CO} \tag{12}$$

Then, the oscillatory component W_{osc} of the hydraulic power is obtained as

$$W_{\mathrm{osc}} = W_{\mathrm{tot}} - W_{\mathrm{mean}} \tag{13}$$

Oscillatory power is typically interpreted as the energy per unit time that is not spent propelling blood forward, or the power wasted because of wave reflections. Recent observations that W_{osc} is a constant fraction of the total hydraulic load even in the presence of RV dysfunction[81] seem to contradict earlier studies showing that chronic RV disease can be associated with an increase in the $W_{\mathrm{osc}}/W_{\mathrm{tot}}$ ratio.[18,35] Since hydraulic power neglects other components of RV power that can also be altered by RV dysfunction, further investigation is necessary to understand whether $W_{\mathrm{osc}}/W_{\mathrm{osc}}$ can be regarded as a reliable surrogate of RV efficiency.

Noninvasive Measurements of RV Function and Efficiency

PV and pressure-flow analyses represent the established clinically applicable tools to assess RV function and efficiency, but they are not ideal for the frequent monitoring of chronic disease. Both methods depend on invasive measurement of pressure in the RV and MPA. If these invasive procedures could be replaced with non-invasive approaches to evaluate RV disease, the benefit would be a significant reduction in the risks required to monitor disease progression and the effect of therapeutic strategies.

Rapid advancement in imaging techniques has been accompanied by a dramatic increase in proposed indices of RV function and efficiency. As soon as these non-invasive physio-markers are established as accurate means to monitor the RV, their translation to clinical practice will revolutionize the management of chronic RV disease. In this section we present a selection of the novel metrics based on non-invasive imaging that appear most promising.

Measurements of Metabolic Efficiency

Measurements of myocardial metabolism can be obtained using positron emission tomography (PET). PET signal from several radiotracers is used to calculate myocardial O_2 consumption, a measure of total cardiac power generation, as the product of myocardial blood flow, myocardial O_2 extraction and arterial O_2 content. An increase in myocardial O_2 consumption for the same cardiac power output results in a reduction of RV mechanical efficiency.[100]

PET has also been used to measure myocardial glucose uptake using ^{18}F-fluorodeoxyglucose (^{18}FDG) as the radiotracer. ^{18}FDG is a glucose analogue that cannot be metabolized and hence accumulates in the cells in proportion to glucose uptake. Since glucose oxidation has a much higher ATP yield than glycolysis, glucose uptake provides a measure of the balance between aerobic and anaerobic metabolism.[66] PET studies with ^{18}FDG have demonstrated a correlation between RV hypertrophy and increased myocardial glucose uptake.[62] These changes reflect a metabolic switch from fatty acids to glucose as the primary energy substrate, and from oxidation to glycolysis as

the primary mechanism.[45] Despite the sensitivity of PET scanning to RV metabolic changes, the predictive value of PET-derived metrics of RV function for morbidity and mortality has yet to be established. For this reason and because of the limited diffusion of PET imaging technology, it is unclear whether PET measurement of RV metabolic efficiency will become a widely used monitoring tool in the clinical setting.

RV Volumes

RV volumes, such as EDV and ESV, provide a basic evaluation of ventricular function. EDV and ESV (usually expressed in mL) represent the maximum and minimum ventricular volume, respectively. An abnormally large EDV can be a sign of filling dysfunction (such as impaired ventricular dilatation). SV is the blood volume ejected in a single heart beat, and is defined as

$$\mathrm{SV} = \mathrm{EDV} - \mathrm{ESV} \tag{14}$$

SV is related to CO, which is the time-averaged flow rate of blood pumped by the heart (either the right or LV, although typically these are the same):

$$\mathrm{CO} = \mathrm{SV} \times \mathrm{HR} \tag{15}$$

where HR is heart rate. The ejection fraction (EF) is defined as

$$\mathrm{EF} = \frac{\mathrm{EDV} - \mathrm{ESV}}{\mathrm{EDV}} \tag{16}$$

and is another important measure of RV function.

RV volumes can be measured invasively during RHC or non-invasively using echocardiography, computed tomography (CT) or MRI. During RHC a thermodilution catheter can be placed in the MPA to estimate RV EF.[22] Alternatively a conductance catheter placed in the RV can measure instantaneous volumes throughout the heart cycle.[20] However, the need for a specialized equipment and software has limited the use of conductance catheters to a small number of research centers. CO is commonly assessed during RHC using either Fick or thermodilution method.[38]

MRI and CT provide better non-invasive measurements of RV volumes than echocardiography. Echocardiographic measurements of RV volumes are based on simplifying assumptions of ventricular shape that, while reasonable in the LV, lead to unacceptably large errors in RV volume estimates. Cardiac MRI is currently the gold standard for measuring RV volumes. It is non-invasive, does not involve ionizing radiation and does not require any geometric assumptions, which makes the method highly accurate. Inter-observer reproducibility is good,[57] although a challenge can be the difficulty separating the RV from the right atrium.[12]

RV Wall Stress and Myocardial Fibrosis

Evaluation of wall stress in relation to increased ventricular afterload is not a new idea, at least in the LV.[36] Under certain geometrical assumptions, Laplace's law can be used to assess wall stresses as a function of intramural pressure and ventricle radius and thickness. Extension of this concept to the RV has been hindered by the complex geometry and the difficulty in estimating wall thickness.[68] Cardiac MRI makes it possible to accurately evaluate RV geometry and wall thickness, nonetheless calculation of wall stress still requires invasive measurement of RV pressure.

Indirect evidence of elevated RV wall stresses can be obtained with delayed contrast enhancement (DCE) measured with cardiac MRI. DCE is due to the slower clearance of the contrast agent gadolinium in necrotic or fibrotic tissues and is therefore observed in sites of myocardial infarction or fibrosis.[52] DCE concentrated in specific locations of the RV tissue can be a marker of non-ischemic RV disease.[52] For instance, DCE in the RV outflow tract correlates with poor EF in patients with repaired tetralogy of Fallot,[63] whereas DCE in the RV insertion points correlates with poor EF and increased RV wall thickness in patients with chronic pulmonary hypertension.[55,76,84] Localized fibrosis is thought to be an indicator of locally elevated wall stresses.[11]

RV Deformation

Measurements of RV motion and deformation have been extensively used to assess RV function. Either MRI or echocardiography can be used with sufficient accuracy, and so the latter has been generally preferred because of the wider availability of echocardiographic equipment in clinical centers.

Accurate RV EF cannot be directly obtained from echocardiographic measurements of RV volumes, and so several indirect methods have been proposed to estimate EF from measurements of RV motion and deformation. RV fractional area change (RV-FAC) can be calculated as the relative difference between end-diastolic and end-systolic RV area, as seen with echocardiography in a four-chamber view. RV-FAC correlates with RV EF and has a strong prognostic value in right heart disease.[5] RV-FAC does not require geometrical assumptions, but inadequate image quality can result in high intra- and inter-observer variability.[72]

Tricuspid annular plane systolic excursion (TAPSE) is a promising method, based on the characteristic displacement of the tricuspid valve during systolic contraction. TAPSE can be measured non-invasively

by M-mode or 2D echocardiography. TAPSE has excellent correlation with RV EF in different types of chronic pulmonary hypertension.[25,29,53] However, one limitation is that TAPSE can be affected by the overall motion of the heart, which can make measurements unreliable when comparing conditions where heart motion is different.[32] Furthermore, TAPSE is reduced to the same degree in patients with either RV dysfunction or LV dysfunction,[50] which limits its prognostic value.

RV strain and strain rate are measurements of myocardial deformation. Both parameters show strong correlation with RV failure.[74] It has been suggested that, at least in some conditions, they are preferable to TAPSE because they do not depend on heart motion.[32] RV strain and strain rate can be measured by either tissue Doppler or speckle tracking echocardiography.[2,3] Also, they can be measured with cardiac MRI tissue tagging techniques, although the RV wall is typically too thin (less than 5 mm) to obtain accurate measurements from MRI.[83]

MRI has been used to measure RV regional transverse motion, which also contributes to RV contraction. In the presence of diastolic RV dysfunction (abnormal filling) the distance between septum and RV free wall (septum-free wall distance; SFD) changes because of the interventricular septal leftward bowing. In one study, MRI measurements of fractional SFD demonstrated stronger correlation with RV EF than MRI-based TAPSE.[43]

Relative Area Change of the Proximal Pulmonary Arteries

The large, proximal, extralobar pulmonary arteries (PAs) distend as an effect of the transmural pressure to accommodate variations in blood flow. Decreased PA compliance is common in diseases associated with PA pressure elevation and can contribute to RV dysfunction. Assessment of PA compliance usually requires invasive measurements of PA pressure. In contrast, the relative area change (RAC) of the proximal PA can be measured non-invasively by MRI,[77,87] echocardiography or computed tomographic (CT) angiography.[69] The RAC is defined as

$$\mathrm{RAC} = \frac{A_{\max} - A_{\min}}{A_{\max}} \tag{17}$$

where $A_{\min}$ and $A_{\max}$ are the minimum and maximum PA cross section area, respectively. The RAC represents an area strain, and as such is not a measure of compliance. However, since the systolic (sPAP) and diastolic pulmonary artery pressure (dPAP) are linearly correlated,[91] the RAC is a valid surrogate of the local arterial stiffness coefficient β, defined as

$$\beta = \frac{\ln(\mathrm{sPAP}/\mathrm{dPAP})}{2\mathrm{RAC}} \tag{18}$$

Recently, the ratio $A_{\min}$/EF has been proposed as a novel noninvasive marker of RV progressive dysfunction.[58] In a large cohort of patients with chronic pulmonary hypertension, $A_{\min}$/EF correlated with elevated mPAP better than RV volumes or RAC. It is yet to be established whether $A_{\min}$/EF can predict RV failure.

RV DYSFUNCTION IN PULMONARY HYPERTENSION

Pulmonary hypertension (PH) is the most common cause of pressure overload in the RV. PH is diagnosed when mPAP, as measured by RHC, is at least 25 mmHg at rest.[27] This broad definition includes several PH subtypes. The most recent classification was proposed at the 4th World Symposium on Pulmonary Hypertension, held in 2008 at Dana Point, and is summarized in Table 1. PAH is an important subtype of PH and originates from a progressive narrowing of the small peripheral PAs due to abnormal muscularization and medial hypertrophy. PAH can be idiopathic, heritable or associated with other diseases, such as connective tissue disease, HIV infection, congenital heart disease and portal hypertension.[86] Distinctive characteristics of idiopathic PAH are neointimal proliferation, obliterative and plexiform lesions. PAH is diagnosed if, in addition to increased mPAP, PCWP is lower than 15 mmHg[7] and all other types of PH have been excluded.

PAH is frequently responsible for proximal PA stiffening[28,51,69,77,90] and RV dysfunction,[9,17,68,97] which have a strong prognostic value for mortality in PAH. Decreased RAC is also correlated with decreased RV EF and increased RV EDV and mass.[87] RV failure is the leading cause of death in PAH.

As a consequence of the PA pressure elevation, the RV has to accommodate an increased afterload. Homeometric autoregulation promotes an increase in RV contractility. In this condition, elevated wall stresses develop in the RV lateral free wall[68] and outflow tract.[85] Increased wall stresses stimulate RV hypertrophy.[85] Stresses can be particularly intense at the RV free wall insertion point, which results in localized RV fibrosis, observed with DCE measurements in several studies on PAH patients (Fig. 6).[55,76,84] In PAH, RV fibrosis has been correlated with elevated mPAP and PVR,[76,84] and RV hypertrophy.[84] At least in early/mild PAH, hypertrophy is beneficial to RV function, as the thicker ventricle is able to generate sufficient pressures to match

TABLE 1. Clinical classification of pulmonary hypertension (Dana Point 2008[86]).

1. PAH
1.1. Idiopathic PAH
1.2. Heritable
1.2.1. BMPR2
1.2.2. ALK1, endoglin (with or without hereditary hemorrhagic telangiectasia)
1.2.3. Unknown
1.3. Drug- and toxin-induced
1.4. Associated with
1.4.1. Connective tissue diseases
1.4.2. HIV infection
1.4.3. Portal hypertension
1.4.4. Congenital heart diseases
1.4.5. Schistosomiasis
1.4.6. Chronic hemolytic anemia
1.5 Persistent pulmonary hypertension of the newborn
1′. Pulmonary veno-occlusive disease (PVOD) and/or pulmonary capillary hemangiomatosis (PCH)
2. Pulmonary hypertension owing to left heart disease
2.1. Systolic dysfunction
2.2. Diastolic dysfunction
2.3. Valvular disease
3. Pulmonary hypertension owing to lung diseases and/or hypoxia
3.1. Chronic obstructive pulmonary disease
3.2. Interstitial lung disease
3.3. Other pulmonary diseases with mixed restrictive and obstructive pattern
3.4. Sleep-disordered breathing
3.5. Alveolar hypoventilation disorders
3.6. Chronic exposure to high altitude
3.7. Developmental abnormalities
4. Chronic thromboembolic pulmonary hypertension (CTEPH)
5. Pulmonary hypertension with unclear multifactorial mechanisms
5.1. Hematologic disorders: myeloproliferative disorders, splenectomy
5.2. Systemic disorders: sarcoidosis, pulmonary Langerhans cell histiocytosis: lymphangioleiomyomatosis, neurofibromatosis, vasculitis
5.3. Metabolic disorders: glycogen storage disease, Gaucher disease, thyroid disorders
5.4. Others: tumoral obstruction, fibrosing mediastinitis, chronic renal failure on dialysis

BMPR2 bone morphogenetic protein receptor type 2, *ALK1* activin receptor-like kinase type 1, *HIV* human immunodeficiency virus.

increased afterload. Measurements of hemodynamic coupling efficiency showed that in mild PAH contractile function can adequately accommodate the increased afterload and η_{vv} is maintained.[78] Non-invasive measurements with MRI have indicated that increased RV mass and RV wall thickness are not strong predictors of mortality in PAH.[97] This finding seems to supports the hypothesis that RV hypertrophy without dilatation (also referred to as concentric hypertrophy) is an adaptive remodeling of the ventricle and does not inevitably lead to RV dysfunction and failure.[68]

In most PAH patients, hypertrophy cannot maintain RV function indefinitely with continued, progressive afterload increases. In severe PAH, E_{es} no longer matches E_a and η_{vv} drops, resulting in ventricular–vascular uncoupling.[46,78] As a consequence of progressive systolic dysfunction, EDV increases and the RV dilates, while adequate SV is maintained by heterometric autoregulation, although again not indefinitely. Increased EDV is a strong predictor of mortality in PAH, as is decreased SV,[97] which suggests that RV failure may begin as heterometric autoregulation fails. RV EF is also closely related to the progression of RV dilatation and has been recognized as a strong predictor of mortality in PAH.[41,96] Therefore, RV dilatation likely represents a maladaptive form of RV remodeling that foreshadows RV failure.

The factors that determine the transition from adaptive hypertrophy to maladaptive remodeling are not clear and probably involve multiple mechanisms active at organ, tissue and cellular levels. The RV energy balance seems to play a role in the progression of RV dysfunction in PAH. In the dilated RV, power consumption is aggravated by the increasing energy required to stretch the RV elastic tissues, leading to a decline in RV efficiency.[100] In addition, the inter-ventricular septum bends leftward as a result of RV dilatation, and the subsequent loss of RV-LV synchronization also contributes to the decrease in RV mechanical efficiency. While imposing an increasing power demand on the RV, PAH also impacts the O_2 supply to the RV, *via* myocardial capillary rarefaction and decreased coronary perfusion pressure.[67] The result is RV ischemia, in other words insufficient O_2 supply to the RV myocardium. Not surprisingly, in PAH patients, RV ischemia is strongly correlated with RV dysfunction.[33]

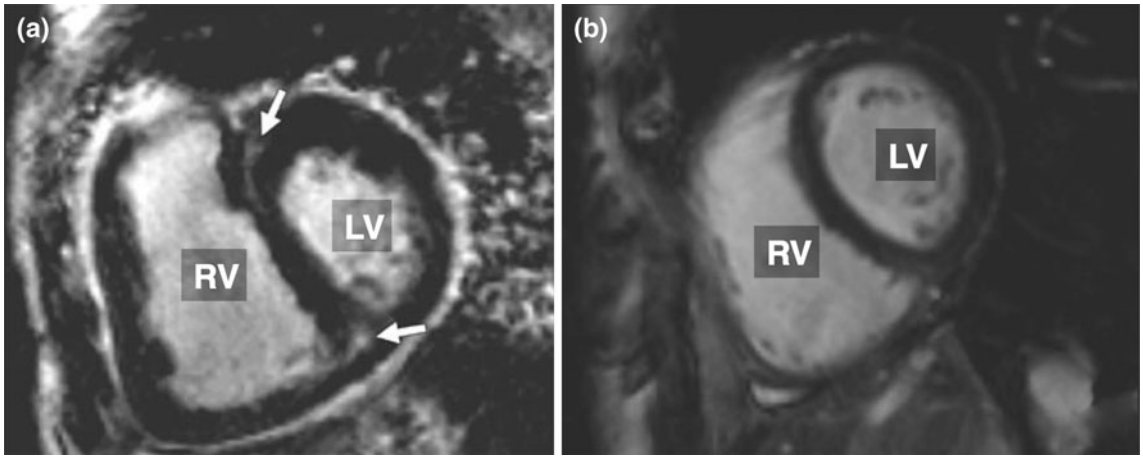

FIGURE 6. MR images collected 10 min after administration of gadolinium contrast in (a) a patient with PAH and (b) a patient with scleroderma but no PH. In the PAH patient, DCE appears as bright areas at the RV free wall insertion points (indicated by the arrows). DCE is absent in the patient without PH. Figure adapted from Shehata et al[84]. Reprinted with permission from the American Journal of Roentgenology.

Invasive and non-invasive methods for measuring RV function and efficiency are essential tools in clinical and preclinical research to help clarify the mechanisms of progressive RV dysfunction and failure in PAH. More work needs to be done to translate these methods into monitoring tools to support clinical management of PAH patients and others with pulmonary vascular disease.

CONCLUDING REMARKS

The study of right heart diseases and mechanisms of response and adaptation of the RV to pathological conditions is recently receiving significant attention. Primary endpoints (RV volumes and pressure, pulmonary vascular resistance) provide limited insight into the mechanisms of RV failure. Hemodynamic coupling of the RV and pulmonary circulation, as well as RV mechanical and metabolic efficiency, are key aspects of cardiopulmonary status. In the RV, the primary challenge for engineers is to develop engineering tools that take into account the complex geometry of the chamber for mechanical analysis and take advantage of the formidable progress in medical imaging to develop non-invasive metrics of RV function and progression of dysfunction to failure. The knowledge accumulated about the mechanics and physiology of the LV cannot be translated, *as is*, to the only apparently similar RV. In recent years, metrics of RV efficiency and ventricular–vascular coupling have been refined, or even redefined, in the light of the distinctive characteristics of the RV. Non-invasive measurements of RV function appear promising to monitor disease progression and support disease-and patient-specific treatment selection. Future research will have to focus on the definition and validation of the most accurate non-invasive markers, *via* a combination of large animal studies and clinical trials. The promise is a significant improvement of patients' life expectancy and quality of life.

ACKNOWLEDGMENTS

The authors gratefully acknowledge funding support from NIH 1R01HL105598 (NCC).

REFERENCES

[1]Abel, F. L. Fourier analysis of left ventricular performance evaluation of impedance matching. *Circ. Res.* 28:119–135, 1971.
[2]Abraham, T. P., V. L. Dimaano, and H.-Y. Liang. Role of tissue Doppler and strain echocardiography in current clinical practice. *Circulation* 116:2597–2609, 2007.
[3]Amundsen, B. H., *et al*. Noninvasive myocardial strain measurement by speckle tracking echocardiography: validation against sonomicrometry and tagged magnetic resonance imaging. *J. Am. Coll. Cardiol.* 47:789–793, 2006.
[4]Anderson, R. H., and S. Y. Ho. What is a ventricle? *Ann. Thorac. Surg.* 66:616–620, 1998.
[5]Antoni, M. L., *et al*. Prognostic value of right ventricular function in patients after acute myocardial infarction treated with primary percutaneous coronary intervention. *Circ. Cardiovasc. Imaging* 3:264–271, 2010.
[6]Baicu, C. F., M. R. Zile, G. P. Aurigemma, and W. H. Gaasch. Left ventricular systolic performance, function, and contractility in patients with diastolic heart failure. *Circulation* 111:2306–2312, 2005.

[7]Barst, R. J., *et al*. Diagnosis and differential assessment of pulmonary arterial hypertension. *J. Am. Coll. Cardiol*. 43:40S–47S, 2004.
[8]Bellofiore, A., *et al*. Impact of acute pulmonary embolization on arterial stiffening and right ventricular function in dogs. *Ann. Biomed. Eng*. 41:195–204, 2013.
[9]Benza, R. L., *et al*. Predicting survival in pulmonary arterial hypertension: insights from the Registry to Evaluate Early and Long-Term Pulmonary Arterial Hypertension Disease Management (REVEAL). *Circulation* 122:164–172, 2010.
[10]Bishop, A., *et al*. Clinical application of the conductance catheter technique in the adult human right ventricle. *Int. J. Cardiol*. 58:211–221, 1997.
[11]Blyth, K. G., *et al*. Contrast enhanced-cardiovascular magnetic resonance imaging in patients with pulmonary hypertension. *Eur. Heart J*. 26:1993–1999, 2005.
[12]Bonnemains, L., *et al*. Assessment of right ventricle volumes and function by cardiac MRI: quantification of the regional and global interobserver variability. *Magn. Reson. Med*. 67:1740–1746, 2012.
[13]Brimioulle, S., P. Wauthy, and R. Naeije. Single-beat evaluation of right ventricular contractility. *Crit. Care Med*. 33:917–918, 2005.
[14]Brimioulle, S., *et al*. Single-beat estimation of right ventricular end-systolic pressure-volume relationship. *Am. J. Physiol. Heart Circ. Physiol*. 284:H1625–H1630, 2003.
[15]Brown, K. A., and R. V. Ditchey. Human right ventricular end-systolic pressure-volume relation defined by maximal elastance. *Circulation* 78:81–91, 1988.
[16]Burkhoff, D., and K. Sagawa. Ventricular efficiency predicted by an analytical model. *Am. J. Physiol. Regul. Integr. Comp. Physiol*. 250:R1021–R1027, 1986.
[17]D'Alonzo, G. E., *et al*. Survival in patients with primary pulmonary hypertension. Results from a national prospective registry. *Ann. Intern. Med*. 115:343–349, 1991.
[18]D'Orio, V., *et al*. Pulmonary impedance and right ventricular–vascular coupling in endotoxin shock. *Cardiovasc. Res*. 38:375–382, 1998.
[19]Daicho, T., *et al*. Possible involvement of mitochondrial energy-producing ability in the development of right ventricular failure in monocrotaline-induced pulmonary hypertensive rats. *J. Pharmacol. Sci*. 111:33–43, 2009.
[20]Danton, M. H. D., *et al*. Right ventricular volume measurement by conductance catheter. *Am. J. Physiol. Heart Circ. Physiol*. 285:H1774–H1785, 2003.
[21]Das, A., R. K. Banerjee, and W. M. Gottliebson. Right ventricular inefficiency in repaired tetralogy of Fallot: proof of concept for energy calculations from cardiac MRI data. *Ann. Biomed. Eng*. 38:3674–3687, 2010.
[22]Dos Santos, I., *et al*. Measurement of ejection fraction with standard thermodilution catheters. *Med. Eng. Phys*. 24:325–335, 2002.
[23]Fisher, M. R., *et al*. Accuracy of Doppler echocardiography in the hemodynamic assessment of pulmonary hypertension. *Am. J. Respir. Crit. Care Med*. 179:615–621, 2009.
[24]Fitzpatrick, J. M., and B. J. Grant. Effects of pulmonary vascular obstruction on right ventricular afterload. *Am. Rev. Respir. Dis*. 141:944–952, 1990.
[25]Forfia, P. R., *et al*. Tricuspid annular displacement predicts survival in pulmonary hypertension. *Am. J. Respir. Crit. Care Med*. 174:1034–1041, 2006.
[26]Fourie, P. R., A. R. Coetzee, and C. T. Bolliger. Pulmonary artery compliance: its role in right ventricular–arterial coupling. *Cardiovasc. Res*. 26:839–844, 1992.
[27]Galiè, N., *et al*. Guidelines for the diagnosis and treatment of pulmonary hypertension the task force for the diagnosis and treatment of pulmonary hypertension of the European Society of Cardiology (ESC) and the European Respiratory Society (ERS), endorsed by the Internati. *Eur. Heart J*. 30:2493–2537, 2009.
[28]Gan, C. T.-J., *et al*. Noninvasively assessed pulmonary artery stiffness predicts mortality in pulmonary arterial hypertension. *Chest* 132:1906–1912, 2007.
[29]Ghio, S., *et al*. Prognostic relevance of the echocardiographic assessment of right ventricular function in patients with idiopathic pulmonary arterial hypertension. *Int. J. Cardiol*. 140:272–278, 2010.
[30]Ghuysen, A., *et al*. Alteration of right ventricular–pulmonary vascular coupling in a porcine model of progressive pressure overloading. *Shock* 29:197–204, 2008.
[31]Giardini, A., and T. A. Tacy. Non-invasive estimation of pressure gradients in regurgitant jets: an overdue consideration. *Eur. J. Echocardiogr*. 9:578–584, 2008.
[32]Giusca, S., *et al*. Deformation imaging describes right ventricular function better than longitudinal displacement of the tricuspid ring. *Heart* 96:281–288, 2010.
[33]Gómez, A., *et al*. Right ventricular ischemia in patients with primary pulmonary hypertension. *J. Am. Coll. Cardiol*. 38:1137–1142, 2001.
[34]Gorcsan, 3rd, J., *et al*. Right ventricular performance and contractile reserve in patients with severe heart failure. Assessment by pressure-area relations and association with outcome. *Circulation* 94:3190–3197, 1996.
[35]Grignola, J. C., F. Ginés, D. Bia, and R. Armentano. Improved right ventricular–vascular coupling during active pulmonary hypertension. *Int. J. Cardiol*. 115:171–182, 2007.
[36]Grossman, W., D. Jones, and L. P. McLaurin. Wall stress and patterns of hypertrophy in the human left ventricle. *J. Clin. Invest*. 56:56–64, 1975.
[37]Gupta, K. B., *et al*. Measurement of end-systolic pressure-volume relations by intra-aortic balloon occlusion. *Circulation* 80:1016–1028, 1989.
[38]Hoeper, M. M., *et al*. Determination of cardiac output by the Fick method, thermodilution, and acetylene rebreathing in pulmonary hypertension. *Am. J. Respir. Crit. Care Med*. 160:535–541, 1999.
[39]Huez, S., S. Brimioulle, R. Naeije, and J.-L. Vachiéry. Feasibility of routine pulmonary arterial impedance measurements in pulmonary hypertension. *Chest* 125:2121–2128, 2004.
[40]Kasner, M., *et al*. Left ventricular dysfunction induced by nonsevere idiopathic pulmonary arterial hypertension: a pressure-volume relationship study. *Am. J. Respir. Crit. Care Med*. 186:181–189, 2012.
[41]Kawut, S. M., *et al*. New predictors of outcome in idiopathic pulmonary arterial hypertension. *Am. J. Cardiol*. 95:199–203, 2005.
[42]Kerbaul, F., *et al*. How prostacyclin improves cardiac output in right heart failure in conjunction with pulmonary hypertension. *Am. J. Respir. Crit. Care Med*. 175:846–850, 2007.
[43]Kind, T., *et al*. Right ventricular ejection fraction is better reflected by transverse rather than longitudinal wall motion in pulmonary hypertension. *J. Cardiovasc. Magn. Reson*. 12:35, 2010.
[44]Kjørstad, K. E., C. Korvald, and T. Myrmel. Pressure–volume-based single-beat estimations cannot predict left ventricular contractility in vivo. *Am. J. Physiol. Heart Circ. Physiol*. 282:H1739–H1750, 2002.

[45]Kolwicz, S. C. J., and R. Tian. Glucose metabolism and cardiac hypertrophy. *Cardiovasc. Res.* 90:194–201, 2011.
[46]Kuehne, T., *et al.* Magnetic resonance imaging analysis of right ventricular pressure-volume loops. *Circulation* 110:2010–2016, 2004.
[47]Lambermont, B., *et al.* Effects of endotoxic shock on right ventricular systolic function and mechanical efficiency. *Cardiovasc. Res.* 59:412–418, 2003.
[48]Lambermont, B., *et al.* Comparison between single-beat and multiple-beat methods for estimation of right ventricular contractility. *Crit. Care Med.* 32:1886–1890, 2004.
[49]Lopaschuk, G. D., *et al.* Myocardial fatty acid metabolism in health and disease. *Physiol. Rev.* 90:207–258, 2010.
[50]López-Candales, A., *et al.* Right ventricular systolic function is not the sole determinant of tricuspid annular motion. *Am. J. Cardiol.* 98:973–977, 2006.
[51]Mahapatra, S., *et al.* Relationship of pulmonary arterial capacitance and mortality in idiopathic pulmonary arterial hypertension. *J. Am. Coll. Cardiol.* 47:799–803, 2006.
[52]Mahrholdt, H., *et al.* Delayed enhancement cardiovascular magnetic resonance assessment of non-ischaemic cardiomyopathies. *Eur. Heart J.* 26:1461–1474, 2005.
[53]Mathai, S. C., *et al.* Tricuspid annular plane systolic excursion is a robust outcome measure in systemic sclerosis-associated pulmonary arterial hypertension. *J. Rheumatol.* 38:2410–2418, 2011.
[54]Matthews, J. C., and V. McLaughlin. Acute right ventricular failure in the setting of acute pulmonary embolism or chronic pulmonary hypertension: a detailed review of the pathophysiology, diagnosis, and management. *Curr. Cardiol. Rev.* 4:49–59, 2008.
[55]McCann, G. P., *et al.* Extent of MRI delayed enhancement of myocardial mass is related to right ventricular dysfunction in pulmonary artery hypertension. *AJR Am. J. Roentgenol.* 188:349–355, 2007.
[56]Monroe, R. G., *et al.* The Anrep effect reconsidered. *J. Clin. Invest.* 51:2573–2583, 1972.
[57]Mooij, C. F., *et al.* Reproducibility of MRI measurements of right ventricular size and function in patients with normal and dilated ventricles. *J. Magn. Reson. Imaging* 28:67–73, 2008.
[58]Moral, S., *et al.* New index alpha improves detection of pulmonary hypertension in comparison with other cardiac magnetic resonance indices. *Int. J. Cardiol.* 161:25–30, 2012.
[59]Morimont, P., *et al.* Effective arterial elastance as an index of pulmonary vascular load. *Am. J. Physiol. Heart Circ. Physiol.* 294:H2736–H2742, 2008.
[60]Nozawa, T., *et al.* Relation between oxygen consumption and pressure-volume area of in situ dog heart. *Am. J. Physiol.* 253:H31–H40, 1987.
[61]O'Rourke, M. F. Vascular impedance in studies of arterial and cardiac function. *Physiol. Rev.* 62:570–623, 1982.
[62]Oikawa, M., *et al.* Increased [18F]fluorodeoxyglucose accumulation in right ventricular free wall in patients with pulmonary hypertension and the effect of epoprostenol. *J. Am. Coll. Cardiol.* 45:1849–1855, 2005.
[63]Oosterhof, T., B. J. M. Mulder, H. W. Vliegen, and A. de Roos. Corrected tetralogy of Fallot: delayed enhancement in right ventricular outflow tract. *Radiology* 237:868–871, 2005.
[64]Overbeek, M. J., *et al.* Right ventricular contractility in systemic sclerosis-associated and idiopathic pulmonary arterial hypertension. *Eur. Respir. J.* 31:1160–1166, 2008.
[65]Pagnamenta, A., *et al.* Early right ventriculo-arterial uncoupling in borderline pulmonary hypertension on experimental heart failure. *J. Appl. Physiol.* 109:1080–1085, 2010.
[66]Peterson, L. R., and R. J. Gropler. Radionuclide imaging of myocardial metabolism. *Circ Cardiovasc Imaging* 3:211–222, 2010.
[67]Piao, L., G. Marsboom, and S. L. Archer. Mitochondrial metabolic adaptation in right ventricular hypertrophy and failure. *J. Mol. Med.* 88:1011–1020, 2010.
[68]Quaife, R. A., *et al.* Importance of right ventricular end-systolic regional wall stress in idiopathic pulmonary arterial hypertension: a new method for estimation of right ventricular wall stress. *Eur. J. Med. Res.* 11:214–220, 2006.
[69]Revel, M.-P., *et al.* Pulmonary hypertension: eCG-gated 64-section CT angiographic evaluation of new functional parameters as diagnostic criteria. *Radiology* 250:558–566, 2009.
[70]Rex, S., *et al.* Effects of inhaled iloprost on right ventricular contractility, right ventriculo-vascular coupling and ventricular interdependence: a randomized placebo-controlled trial in an experimental model of acute pulmonary hypertension. *Crit. Care* 12:R113, 2008.
[71]Rich, J. D., *et al.* Inaccuracy of Doppler echocardiographic estimates of pulmonary artery pressures in patients with pulmonary hypertension: implications for clinical practice. *Chest* 139:988–993, 2011.
[72]Roberts, J. D., and P. R. Forfia. Diagnosis and assessment of pulmonary vascular disease by Doppler echocardiography. *Pulm. Circ.* 1:160–181, 2011.
[73]Rondelet, B., *et al.* Sildenafil added to sitaxsentan in overcirculation-induced pulmonary arterial hypertension. *Am. J. Physiol. Heart Circ. Physiol.* 299:H1118–H1123, 2010.
[74]Sachdev, A., *et al.* Right ventricular strain for prediction of survival in patients with pulmonary arterial hypertension. *Chest* 139:1299–1309, 2011.
[75]Santamore, W. P., and L. J. Dell'Italia. Ventricular interdependence: significant left ventricular contributions to right ventricular systolic function. *Prog. Cardiovasc Dis.* 40:289–308, 1998.
[76]Sanz, J., *et al.* Prevalence and correlates of septal delayed contrast enhancement in patients with pulmonary hypertension. *Am. J. Cardiol.* 100:731–735, 2007.
[77]Sanz, J., *et al.* Evaluation of pulmonary artery stiffness in pulmonary hypertension with cardiac magnetic resonance. *JACC Cardiovasc. Imaging* 2:286–295, 2009.
[78]Sanz, J., *et al.* Right ventriculo-arterial coupling in pulmonary hypertension: a magnetic resonance study. *Heart* 98:238–243, 2012.
[79]Saouti, N., N. Westerhof, P. E. Postmus, and A. Vonk-Noordegraaf. The arterial load in pulmonary hypertension. *Eur. Respir. Rev.* 19:197–203, 2010.
[80]Saouti, N., *et al.* RC time constant of single lung equals that of both lungs together: a study in chronic thromboembolic pulmonary hypertension. *Am. J. Physiol. Heart Circ. Physiol.* 297:H2154–H2160, 2009.
[81]Saouti, N., *et al.* Right ventricular oscillatory power is a constant fraction of total power irrespective of pulmonary artery pressure. *Am. J. Respir. Crit. Care Med.* 182:1315–1320, 2010.
[82]Sheehan, F., and A. Redington. The right ventricle: anatomy, physiology and clinical imaging. *Heart* 94:1510–1515, 2008.
[83]Shehata, M. L., *et al.* Myocardial tissue tagging with cardiovascular magnetic resonance. *J. Cardiovasc. Magn. Reson.* 11:55, 2009.

[84]Shehata, M. L., *et al*. Myocardial delayed enhancement in pulmonary hypertension: pulmonary hemodynamics, right ventricular function, and remodeling. *AJR Am. J. Roentgenol*. 196:87–94, 2011.
[85]Simon, M. A., *et al*. Phenotyping the right ventricle in patients with pulmonary hypertension. *Clin. Transl. Sci*. 2:294–299, 2009.
[86]Simonneau, G., *et al*. Updated clinical classification of pulmonary hypertension. *J. Am. Coll. Cardiol*. 54:S43–S54, 2009.
[87]Stevens, G. R., *et al*. RV dysfunction in pulmonary hypertension is independently related to pulmonary artery stiffness. *JACC Cardiovasc. Imaging* 5:378–387, 2012.
[88]Suga, H., and K. Sagawa. Instantaneous pressure-volume relationships and their ratio in the excised, supported canine left ventricle. *Circ. Res*. 35:117–126, 1974.
[89]Sunagawa, K., W. L. Maughan, D. Burkhoff, and K. Sagawa. Left ventricular interaction with arterial load studied in isolated canine ventricle. *Am. J. Physiol*. 245:H773–H780, 1983.
[90]Swift, A. J., *et al*. Pulmonary artery relative area change detects mild elevations in pulmonary vascular resistance and predicts adverse outcome in pulmonary hypertension. *Invest. Radiol*. 47:571–577, 2012.
[91]Syyed, R., *et al*. The relationship between the components of pulmonary artery pressure remains constant under all conditions in both health and disease. *Chest* 133:633–639, 2008.
[92]Tabima, D. M., T. A. Hacker, and N. C. Chesler. Measuring right ventricular function in the normal and hypertensive mouse hearts using admittance-derived pressure-volume loops. *Am. J. Physiol. Heart Circ. Physiol*. 299:H2069–H2075, 2010.
[93]Ten Brinke, E. A., *et al*. Single-beat estimation of the left ventricular end-systolic pressure-volume relationship in patients with heart failure. *Acta Physiol. (Oxf.)* 198:37–46, 2010.
[94]Timmer, S. A. J., *et al*. Determinants of myocardial energetics and efficiency in symptomatic hypertrophic cardiomyopathy. *Eur. J. Nucl. Med. Mol. Imaging* 37:779–788, 2010.
[95]Tuder, R. M., L. A. Davis, and B. B. Graham. Targeting energetic metabolism: a new frontier in the pathogenesis and treatment of pulmonary hypertension. *Am. J. Respir. Crit. Care Med*. 185:260–266, 2012.
[96]Van de Veerdonk, M. C., *et al*. Progressive right ventricular dysfunction in patients with pulmonary arterial hypertension responding to therapy. *J. Am. Coll. Cardiol*. 58:2511–2519, 2011.
[97]Van Wolferen, S. A., *et al*. Prognostic value of right ventricular mass, volume, and function in idiopathic pulmonary arterial hypertension. *Eur. Heart J*. 28:1250–1257, 2007.
[98]Voelkel, N. F., *et al*. Right ventricular function and failure: report of a National Heart, Lung, and Blood Institute working group on cellular and molecular mechanisms of right heart failure. *Circulation* 114:1883–1891, 2006.
[99]Wauthy, P., *et al*. Right ventricular adaptation to pulmonary hypertension: an interspecies comparison. *Am. J. Physiol. Heart Circ. Physiol*. 286:H1441–H1447, 2004.
[100]Wong, Y. Y., *et al*. Right ventricular failure in idiopathic pulmonary arterial hypertension is associated with inefficient myocardial oxygen utilization. *Circ. Heart Fail*. 4:700–706, 2011.